Inorganica Chimica Acta 378 (2011) 87–94

Contents lists available at SciVerse ScienceDirect

Inorganica Chimica Acta

journal homepage: www.elsevier.com/locate/ica

Functional models for enzyme–substrate adducts of catechol dioxygenase enzymes: The Lewis basicity of facially coordinating tridentate phenolate ligands tunes the rate of dioxygenation and product selectivity

Kusalendiran Visvaganesan, Somasundaram Ramachitra, Mallayan Palaniandavar *

Centre for Bioinorganic Chemistry, School of Chemistry, Bharathidasan University, Tiruchirapalli 620 024, India

ARTICLE INFO

Article history:
Received 25 March 2011
Received in revised form 22 July 2011
Accepted 11 August 2011
Available online 22 August 2011

Keywords:
Catechol dioxygenase
Synthetic model
Iron(III)–catecholate adduct
Dioxygenation
Regioselectivity

ABSTRACT

A few iron(III) 3,5-di-*tert*-butylcatecholate (DBC^{2-}) adducts of the type [Fe(L)(DBC)(CH_3OH)], where L is a tridentate substituted monophenolate ligand such as 2-((*N*-benzylpyrid-2-ylmethylamino)methyl)phenol (H(L1)), 2-((*N*-benzylpyrid-2-ylmethylamino)-methyl)-4,6-dimethylphenol (H(L2)), 2-((*N*-benzylpyrid-2-ylmethylamino)methyl)-4,6-di-*tert*-butylphenol (H(L3)) and 2-((*N*-benzylpyrid-2-ylmethylamino) methyl)-4-nitrophenol (H(L4)), have been isolated and characterized by elemental and ESI-MS analysis. The spectral and electrochemical properties and dioxygenase activities of the adducts have been studied in methanol solution. Upon varying the substituents on the phenolate ring from electron-releasing to electron-withdrawing, the redox potential of DBSQ/DBC^{2-} couple is shifted to a more positive value indicating an increase in covalency of iron(III)–catecholate bonds. All the complexes elicit cleavage of DBC^{2-} using molecular oxygen to afford both intra- (I) and extradiol (E) cleavage products with the product selectivity (E/I) varying in the range 0.3–1.9. Interestingly, the incorporation of electron-withdrawing substituents facilitates the regioselective extradiol cleavage of catechol while that of electron-releasing substituents facilitate the regioselective intradiol cleavage.

1. Introduction

Ring opening of dihydroxy aromatic compounds is the most significant single step in the bacterial assimilation of carbon from aromatics [1]. Catechol dioxygenase enzymes in aerobic bacteria catalyze almost exclusively the ring opening using molecular oxygen and two atoms of molecular oxygen are inserted. They are classified into two major groups, namely, the intra- and extradiol-cleaving dioxygenases on the basis of regiospecificity of ring cleavage (Scheme 1) [2–4]. The intradiol dioxygenases contain iron(III) center ligated by two histidine residues, two tyrosine residues and a solvent derived molecule and catalyze the cleavage of the catechol ring between two hydroxylated carbon–carbon double bond [5–10]. On the other hand, the extradiol-cleaving dioxygenases contain iron(II) ligated by 2-His-1-carboxylate facial-triad motif and two water molecules and catalyze the cleavage adjacent to the hydroxylated carbon-carbon double bond [11–16]. The reason for different metal ion (+2 or +3 oxidation state) requirement of the two families of the enzymes, however, remains a mystery in the enzymatic pathway [17,18]. Each family of the enzyme is quite specific for yielding the respective reaction products with a range of substrates and activates either O_2 or the catecholate substrate to overcome the kinetic barrier depending upon their spins.

A plenty of iron(III)/iron(II) complexes of tri- and tetradentate ligands containing pyridine/imidazole/pyrazole/carboxylate and/or phenolate moieties have been reported as structural and functional models for catechol dioxygenase enzymes [19–44]. Most of the model complexes end up with intradiol cleavage products upon interacting them with catechol and O_2 [19–29]. Though iron(II) center is present in the active site of extradiol-cleaving enzymes, small molecule synthetic analogs containing iron(III) also cleave catechols into their extradiol cleavage products [17,31–44]. So attention has been shifted to isolate and study iron(III) complexes as functional models for extradiol-cleaving catechol dioxygenase enzymes [17,31–44]. The iron(III) complexes of 1,4,7-triazacyclononane (TACN) and hydridotris(3,5-diisopropyl-1-pyrazolyl)borate (Tp_2^{ir}) [33–35,45] have been shown to convert catechol into 30–97% extradiol cleavage products. In contrast, the iron(III) complex of the meridionally coordinated tridentate ligand 2,2′,6,2″-terpyridine (tpy) yields mainly the oxidized quinone and intradiol cleavage (20%) products [35,39]. Recently, Gebbink and co-workers have isolated [40] iron(II)– and iron(III)–catecholate complexes of a new family of substituted 3,3-bis(1-alkylimidazol-2-yl)propionate ligands to mimic the structure as well as function of extradiol-cleaving catechol dioxygenases but obtained both extra- (E) and intradiol (I) cleavage products with 1:1 product selectivity (E/I).

* Corresponding author. Tel.: +91 431 2407125; fax: +91 431 2407043.
E-mail addresses: palaniandavarm@gmail.com, palanim51@yahoo.com (M. Palaniandavar).

0020-1693/$ - see front matter © 2011 Elsevier B.V. All rights reserved.
doi:10.1016/j.ica.2011.08.025

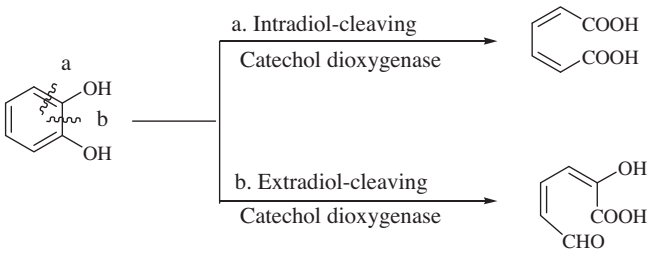

Scheme 1. Mode of cleavage of catechol dioxygenases.

In our laboratory, we have isolated and studied 1:1 iron(III) complexes of several tri- [21,27,39,42–44,46] and tetradentate [30,38] ligands with an aim to mimic the extradiol-cleaving enzymes. We have observed an increase in yield of the cleavage product with increase in Lewis acidity of iron(III) center [46]. Very recently, we have observed the formation of both intra- and extradiol cleavage products upon interacting a series of iron(III) complexes of the type $[Fe(L)Cl_3]$, where L = *N*-alkyl substituted bis(pyrid-2-ylmethyl)amine and (pyrid-2-ylmethyl)ethylenediamine, with H_2DBC under O_2 atmosphere [42,43]. We found that the regioselectivity in catechol cleavage is remarkably tuned by the central as well as terminal *N*-alkyl groups of the facially coordinating tridentate ligands [42,43]. Very interestingly, we have achieved the selective formation of extradiol cleavage products (84–94%) in organized assemblies for the iron(III) complex of the facially coordinating bis(pyrid-2-ylmethyl)amine ligand [47]. All these studies clearly show that the presence of a vacant or solvent coordinated site on the iron(III) center and facial coordination of tridentate ligands are essential to achieve extradiol cleavage products [34,42–44,48]. Previously, we have isolated and studied iron(III) complexes of the type $[Fe(L)Cl_2]$, where L is tridentate monophenolate ligands with an aim to mimic structure and function of protocatechuate-3,4-dioxygenase (3,4-PCD) and catechol-1,2-dioxygenase (1,2-CTD) enzymes [21,46]. Ogo et al. have shown that the adduct [Fe(L)(DBC)Cl], where H(L) = 2-(*N*-benzyl-*N*-pyrid-2-ylmethyl)aminophenol afforded, in spite of the facial coordination of the ligand to iron(III), intradiol cleavage (52%) and oxidized (45%) products upon reacting it with O_2 in DMF solvent [29] and only intradiol cleavage products (97%), even after removal of the coordinated chloride ion in the adduct. So, in continuation of our studies to devise extradiol-cleaving mimics, we have now isolated DBC^{2-} adducts of iron(III) complexes of a few 2NO ligands (H(L1)–H(L4), Scheme 2) containing differently substituted phenolate moieties as models for PCA-bound (PCA = protocatechuic acid) form of 3,4-PCD enzymes. We intend to systematically study the effect of Lewis acidity of the iron(III) center, as modified by the different substituents on the phenolate moiety in the primary ligands, on the regioselectivity of catechol ring cleavage in methanol solvent. Interestingly, we have found that the electron-releasing substituents such as methyl and *tert*-butyl groups on the phenolate ring enhance the yield of intradiol cleavage products while the electron-withdrawing NO_2 group enhances the yield of extradiol cleavage products.

2. Experimental

2.1. Materials

The chemicals benzylamine, pyridine-2-carboxaldehyde, sodium borohydride, 3,4-di-*tert*-butylcatechol, 2,4-dimethylphenol, 2,4-di-*tert*-butylphenol, ferric perchlorate hexahydrate, picolylchloride hydrochloride and 3,5-di-*tert*-butylcatechol (Aldrich), 36% formaldehyde, piperidine, salicylaldehyde, potassium carbonate, sodium sulfate, diethylether and dichloromethane (Merck, India) were used as received. The commercial solvents were distilled and then used for the preparation of the ligands and complexes. The supporting electrolyte tetra-*N*-butylammonium perchlorate was recrystallized twice from aqueous ethanol.

2.2. Physical measurements

Elemental analyses were performed on a Perkin Elmer Series II CHNS/O analyzer 2400. ^1H NMR spectra were recorded on a Bruker 400 MHz NMR spectrometer. ESI-MS analysis was performed on a Q-TOF micromass (YA-105) spectrometer. Electronic spectral measurements in methanol solutions of the iron–DBC^{2-} complexes were made with an Agilent 8453 diode array spectrophotometer. Cyclic voltammetry (CV) and differential pulse voltammetry (DPV) were performed at 25.0 ± 0.2 °C using a three-electrode cell configuration. A platinum sphere, a platinum plate and $Ag(s)/AgNO_3$ were used as working, auxiliary and reference electrodes respectively. The $Ag(s)/Ag^+$ reference electrode consists of a Ag wire immersed in a solution of $AgNO_3$ (0.01 M) and tetra-*N*-butylammonium perchlorate (0.1 M) in an acetonitrile placed in a tube fitted with a vycor plug. The instruments utilized included an EG & G PAR 273 Potentiostat/Galvanostat and P-IV pentium computer along with EG & G M270 software to carry out the experiments and to acquire the data. The temperature of the electrochemical cell was maintained by a cryocirculator (HAAKE D8-G). The $E_{1/2}$ observed under identical conditions for Fc/Fc^+ couple in an acetonitrile was 0.10 V with respect to $Ag(s)/Ag^+$ reference electrode. The experimental solutions were deoxygenated by bubbling research grade nitrogen and an atmosphere of nitrogen was maintained over the solution during measurement. The redox potential ($E_{1/2}$) was calculated from the anodic (E_{pa}) and cathodic peak (E_{pc}) potentials of CV traces as $(E_{pa} + E_{pc})/2$. The redox potentials were also estimated from the DPV peak potentials E_p using the relation,

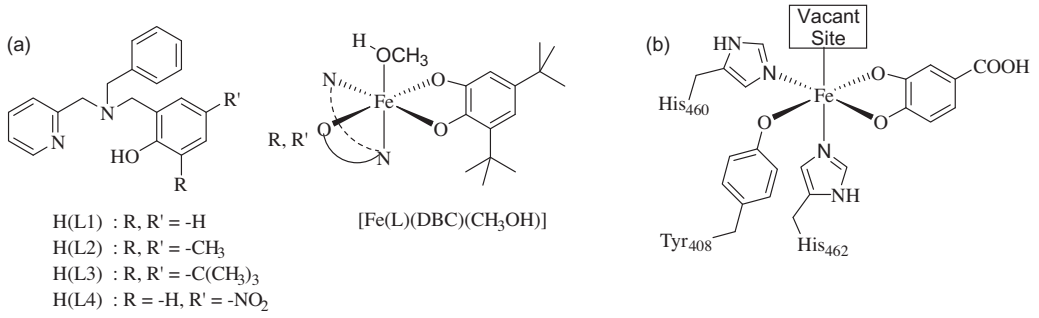

Scheme 2. (a) Schematic drawings of tridentate phenolate ligands and their iron(III)–catecholate adducts. (b) Active site structure of PCA-bound form of 3,4-PCD enzyme.

$$E_{1/2} = E_p + \Delta E/2$$

where $E_{1/2}$ is the equivalent of the average of E_{pc} and E_{pa} in CV experiments and ΔE is the pulse amplitude.

The products were analyzed by using Hewlett Packard (HP) 6890 Gas Chromatograph (GC) series equipped with a FID detector and a HP-5 capillary column (30 m × 0.32 mm × 2.5 μm) with the following temperature program: initial temperature, 50 °C; heating rate 5 °C min^{-1}; final temperature 250 °C; injector temperature 150 °C; and FID temperature 280 °C. GC–MS analysis was performed on a Perkin-Elmer Clarus 500 GC–MS instrument using a PE-5 (HP-5 equivalent) capillary column under conditions that are identical to that used for GC analysis.

2.3. Syntheses of ligands

2.3.1. 2-((N-Benzylpyrid-2-ylmethylamino)methyl)phenol H(L1)

This ligand was synthesized in two steps [49]. The first step in the synthesis was the preparation of *N*-benzylaminomethylphenol which was then reacted with 2-chloromethylpyridine in the second step to obtain the ligand H(L1).

2.3.1.1. Step 1. Synthesis of N-benzylaminomethylphenol. A solution of benzylamine (0.54 g, 5.0 mmol) in 4 mL ethanol and 99% salicylaldehyde (0.62 g, 5.0 mmol) in 4 mL ethanol were mixed. Heat was evolved and the color darkened. The solution was stirred for 12 h and boiled gently 30 min. Then 7.5 mmol of sodium borohydride was added at 0 °C. The mixture was stirred overnight and rotaevaporated. Then it was extracted by CH_2Cl_2 and dried by Na_2SO_4. Yield 0.90 g (85%).

2.3.1.2. Step 2. Synthesis of ligand H(L1). To a solution of *N*-benzylaminomethylphenol (0.90 g, 4.2 mmol) and Et_3N (585 μL, 4.2 mmol) in 10 mL of ethylacetate was added 10 mL of an ethanolic solution of 2-chloromethylpyridine obtained by neutralization of the monohydrochloride (0.69 g, 4.2 mmol) with a 10% excess of a 2 mL saturated aqueous K_2CO_3 solution with vigorous stirring. The mixture was allowed to stir at room temperature for 5 days. After filtration, the solvent was removed under reduced pressure to give yellowish oil. To this was added 20 mL of ethylacetate, the mixture was filtered and the volume of filtrate was reduced to approximately 5 mL by rotary evaporation. The remaining solution was extracted with dichloromethane and dried over Na_2SO_4. Yield 1.26 g (99%). ^{1}H NMR (200 MHz, $CDCl_3$): δ 8.52 (dd, 1H), 7.90–8.00 (m, 2H), 6.6–7.2 (m, 10H), 3.95 (s, 2H), 3.80 (s, 2H), 3.72 (s, 2H).

2.3.2. 2-((N-Benzylpyrid-2-ylmethylamino)methyl)-4,6-dimethylphenol H(L2)

This ligand was synthesized in two steps by a modified procedure reported already [50,51]. The first step in the synthesis was the preparation of *N*-benzylaminomethylpyridine which was then reacted with 2,4-dimethylbutylphenol in the second step to obtain the ligand (L2).

2.3.2.1. Step 1. N-Benzylaminomethylpyridine. A solution of benzylamine (0.54 g, 5.0 mmol) in 4 mL ethanol and pyridine-2-carboxyaldehyde (0.54 g, 5.0 mmol) in 4 mL ethanol were mixed. Heat was evolved and the color darkened. The solution was stirred for 12 h and boiled gently for 30 min. Then 7.5 mmol of sodium borohydride was slowly added with stirring at 0 °C. The mixture was stirred overnight and rotaevaporated. Then it was extracted by CH_2Cl_2 and dried by Na_2SO_4. Yield 0.95 g (96%).

2.3.2.2. Step 2. 2-((N-Benzylpyrid-2-ylmethylamino)methyl)-4,6-dimethylphenol H(L2). A solution of 2,4-dimethylphenol (0.61 g, 5.0 mmol), *N*-benzylaminomethylpyridine (0.99 g, 5.0 mmol), and 36% aqueous formaldehyde (532 μL, 7.5 mmol) in methanol (10 mL) was stirred at room temperature for 3 days. The mixture was cooled in the freezer overnight, filtered and washed thoroughly with ice cold methanol to give the ligand L1 as colorless powder which could be further purified by recrystallization from methanol. The crude product was used for complex preparation without further purification. Yield 1.55 g (93%). ^{1}H NMR (200 MHz, $CDCl_3$): δ 7.6–8.1 (m, 2H), 6.5–7.3 (m, 9H), 3.82 (s, 2H), 3.71 (s, 2H), 3.65 (s, 2H), 2.2 (s, 3H), 1.9 (s, 3H).

2.3.3. 2-((N-Benzylpyrid-2-ylmethylamino)methyl)-4,6-di-tert-butylphenol H(L3)

This ligand was synthesised as reported earlier [52–54]. Yield 1.97 g (95%). ^{1}H NMR (200 MHz, $CDCl_3$): δ 7.3–7.7 (m, 2H), 6.6–7.2 (m, 9H), 3.84 (s, 2H), 3.74 (s, 2H), 3.69 (s, 2H), 1.3 (s, 9H), 1.1 (s, 9H).

2.3.4. 2-((N-Benzylpyrid-2-ylmethylamino)methyl)-4-nitrophenol H(L4)

To a cold tetrahydrofuran solution (15 mL) containing *N*-benzylaminomethylpyridine (0.79 g, 4.0 mmol) and triethylamine (557 μL) was added dropwise 2-chloromethyl-4-nitrophenol (0.75 g, 4.0 mmol) in tetrahydrofuran (10 mL) with rapid stirring. The mixture was allowed to warm to room temperature, and then heated to reflux for 4 h. After rotaevaporation, the ligand 2-((*N*-benzylpyrid-2-ylmethylamino)methyl)-4-nitrophenol as an yellow oil. The product was used as such for the complex preparation. Yield 1.38 g (98%). ^{1}H NMR (200 MHz, $CDCl_3$): δ 8.52 (dd, 1H), 7.90–8.00 (m, 2H), 7.5–7.6 (dt, 1H), 6.6–7.6 (m, 8H), 3.80 (s, 2H), 2.20 (s, 2H), 1.85 (s, 2H).

2.4. Synthesis of mononuclear iron(III)–DBC^{2-} complexes

2.4.1. [Fe(L1)(DBC)(CH_3OH)] **1**

To a methanolic solution (4 mL) of $Fe(ClO_4)_3{\cdot}6H_2O$ (17.0 mg, 0.5 mmol), was added a methanolic solution (4 mL) of ligand L1 (0.5 mmol) pretreated with an equivalent amount of piperidine under nitrogen atmosphere then 0.5 mmol of H_2DBC pretreated with an equivalent amount of piperidine in methanol (3 mL) was added and stirred for 30 min. The resulting solution was layered with hexane and kept under 4 °C, after 2 days dark purple colored complex was obtained. Yield 0.22 g (73%). *Anal.* Calc. for $C_{35}H_{43}FeN_2O_4$: C, 68.74; H, 7.09; N, 4.58. Found: C, 68.64; H, 7.19; N, 4.51%. ESI-MS m/z = 580.22 $FeC_{34}H_{39}N_2O_3^+$.

2.4.2. [Fe(L2)(DBC)(CH_3OH)] **2**

This complex was isolated as a dark purple colored product in a manner analogous to that described for isolating [Fe(L1)(DBC)] using L2 as ligand. Yield 0.21 g (68%). *Anal.* Calc. for $C_{37}H_{47}FeN_2O_4$: C, 69.48; H, 7.41; N, 4.38. Found: C, 69.42; H, 7.35; N, 4.32%. ESI-MS m/z = 607.25 $[FeC_{36}H_{43}N_2O_3]^+$.

2.4.3. [Fe(L3)(DBC)(CH_3OH)] **3**

Complex **3** was prepared by using the procedure employed for [Fe(L1)(DBC)]. Yield 0.26 g (75%). *Anal.* Calc. for $C_{43}H_{59}FeN_2O_4$: C, 71.36; H, 8.22; N, 3.87. Found: C, 71.26; H, 8.30; N, 3.82%. ESI-MS, m/z = 691.32 $[C_{42}H_{55}FeN_2O_3]^+$.

2.4.4. [Fe(L4)(DBC)(CH_3OH)] **4**

This complex was prepared by using the procedure adopted for [Fe(L1)(DBC)]. Yield 0.24 g (76%). *Anal.* Calc. for $C_{35}H_{42}FeN_3O_6$: C, 64.03; H, 6.45; N, 6.40. Found: C, 64.18; H, 6.23; N, 6.45%. ESI-MS m/z = 624.20 $FeC_{34}H_{38}N_3O_5^+$.

2.5. Reactivity studies

The following typical procedure was employed to study the dioxygenases activity of model compounds. A solution of

iron(III)–DBC^{2-} adduct (0.05 mmol) was left in contact with oxygen at room temperature for 3 days. The solvent was then removed under vacuum at 35 °C and the resultant residue was acidified with HCl to pH 3. The organic compounds were extracted from the aqueous solution with diethylether, dried over Na_2SO_4, and then rotaevaporated. The product mixture was then subjected to GC–MS and GC analysis.

3. Results and discussion

3.1. Synthesis of ligands and iron(III)–DBC^{2-} adducts

The linear tridentate monophenolate ligands H(L1)–H(L4) were synthesized according to known procedures [49–54], which involve reductive amination and Mannich base condensation. The N–H hydrogen atom of *N*-benzylaminomethylpyridine can be considered to have been substituted with differently substituted phenolic moieties to give H(L1)–H(L4). The ligand H(L1) was synthesized by reductive amination of salicylaldehyde and benzylamine using sodium borohydride as the reducing agent, followed by reaction with picolylchloride hydrochloride in presence of a base. The ligands H(L2) and H(L3) were prepared by reductive amination of pyridine-2-carboxaldehyde and benzylamine using sodium borohydride as reducing agent followed by Mannich base condensation of the product *N*-benzylaminomethylpyridine with the corresponding phenol and formaldehyde. The ligand H(L4) was synthesized by reacting 2-chloromethyl-4-nitrophenol with *N*-benzylaminomethylpyridine in presence of one equiv. of triethylamine. Attempts to isolate the mononuclear iron(III) complexes of the phenolate ligands failed to yield well-defined products. So, in this study we have isolated the DBC^{2-} adducts (**1**–**4**) of the iron(III) complexes in good yields by reacting the iron(III) complexes generated by mixing equimolar amounts of $Fe(ClO_4)_3{\cdot}6H_2O$, the ligand and one equivalent of piperidine and then treating with H_2DBC pretreated with two equivalents of piperidine in methanol under nitrogen atmosphere (Scheme 2). Based on the elemental analysis all of the present adducts are formulated as [Fe(L)(DBC)(CH_3OH)], which is supported by ESI-MS analysis (Fig. 1), which reveals the presence of $[Fe(L)(DBC)]^{+}$ species for all the adducts, the coordinated solvent molecule being detached from the coordination sphere in the gas phase [55]. Also, it is interesting to note that the 2NO ligands are facially bound to iron(III). The electronic environment around iron(III) center of the present adducts closely mimics the intradiol-cleaving 3,4-PCD enzyme adducts (Scheme 2) and is expected to confer interesting spectral and chemical properties. The vacant site on iron(III) center of the adducts is possibly the site for molecular oxygen binding during oxygenation. The differently substituted phenolic moieties on the ligands are expected to impose varying steric and electronic effects on the iron(III) center and hence the reactivity of the adducts with molecular oxygen.

3.2. Electronic absorption spectra of iron(III)–DBC^{2-} adducts

The absorption spectral data of the present iron(III)–catecholate adducts are collected in Table 1 and a typical electronic absorption spectrum is displayed in Fig. 2. The electronic spectra of **1**–**4** in methanol are dominated by two moderately intense absorption bands in the regions 400–480 and 600–790 nm, which are characteristic of catecholate-to-iron(III) charge-transfer bands [19–28]. The two LMCT bands are attributed to catecholate-to-iron(III) LMCT transitions involving two different catecholate frontier orbitals and $d\pi^*$ orbital of iron(III) center. The energies of the low-energy LMCT band follow the trend **3** > **2** > **1** > **4** indicating that the Lewis acidity of iron(III) center and hence the covalency of iron(III)–catecholate bond increases along this series [42–44]. Thus, upon incorporating the electron-releasing *tert*-butyl groups on the phenolate ring in **1** to obtain **3**, the electron density on iron(III) center increases, the iron(III) $d\pi^*$ orbital is destabilized [19,42,56] and hence the energy gap between the $d\pi^*$ orbital and the catecholate orbitals increases leading to a large blue-shift (160 nm) of the LMCT band. Similarly, as expected, on incorporating the methyl groups to obtain **2**, a much lower blue-shift (20 nm) is observed. On the other hand, on incorporating the electron-withdrawing group $-NO_2$ on the phenolate ring in **1** to obtain **4**, the Lewis acidity of the iron(III) center and

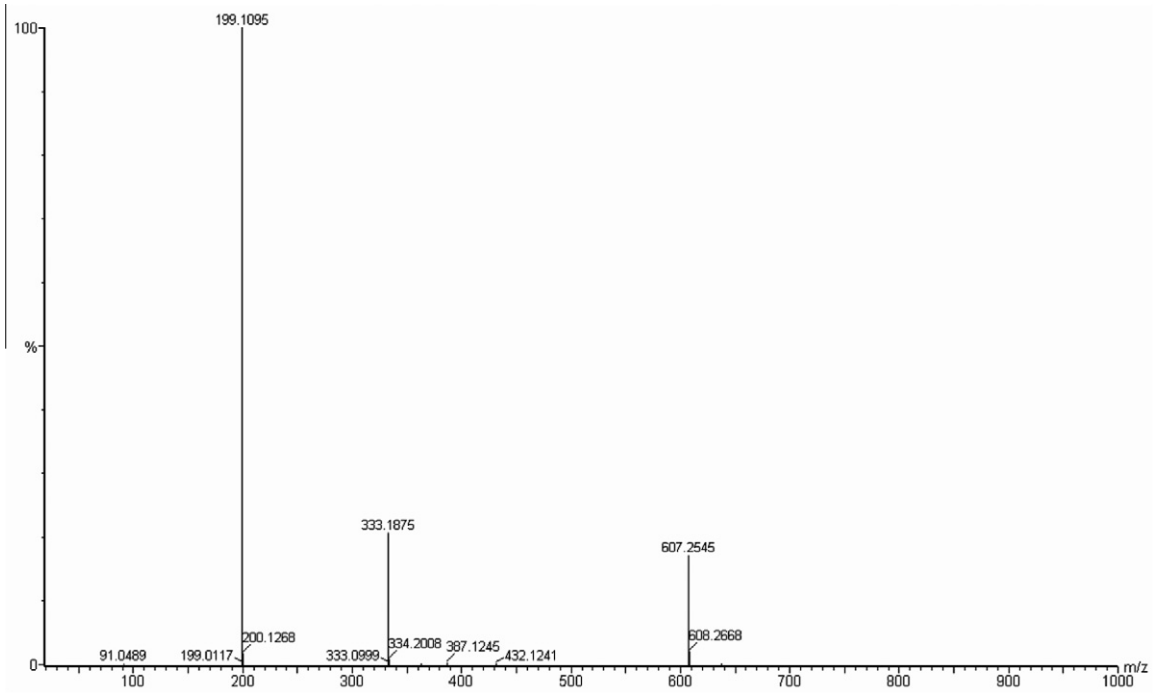

Fig. 1. Electrospray ionization-mass spectrum of complex **2** in methanol.

Table 1
Electronic spectral data (λ_{max} in nm; ε_{max} in $M^{-1}\,cm^{-1}$ in paranthesis) for iron(III)–DBC^{2-} adducts[a] in methanol solution.

Complex	λ_{max} nm (ε_{max} $M^{-1}\,cm^{-1}$)
[Fe(L1)(DBC)(CH_3OH)]	462 (2600)
	758 (2910)
[Fe(L2)(DBC)(CH_3OH)]	472 (2210)
	740 (2375)
[Fe(L3)(DBC)(CH_3OH)]	409 (1430)
	596 (1290)
[Fe(L4)(DBC)(CH_3OH)]	476 (1345)
	787 (1970)

[a] Concentration iron(III)–DBC adducts, 4×10^{-4} M.

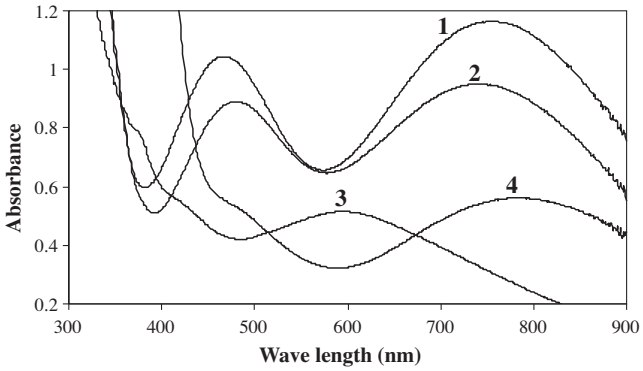

Fig. 2. Electronic absorption spectra of iron–DBC adducts **1**–**4** (2×10^{-4} M) in methanol solution.

hence the covalency of iron(III)–catecholate bond increases leading to the red-shift (47 nm) of the LMCT band. Hence, the position of the low-energy LMCT band exhibits a remarkable dependence on the Lewis basicity of the phenolate ligands, as modified by the phenolate ring substituents and reflects the covalency of the iron(III)–catecholate bonds as modified by the tridentate ligands. Upon adding *N*-methylimidazole (*N*-MeIm) or pyridine in excess, the low-energy LMCT band of iron(III)–DBC^{2-} adducts are shifted to higher energies (4–12 nm) with decrease in absorptivity for **1**–**4**, which is mainly due to the increase in electron density on the iron(III) center by coordination of *N*-MeIm [46]. This suggests that a labile coordination site is available on iron(III) center of the present iron (III)–DBC^{2-} adducts, which may be utilized for O_2 binding during oxygenation.

3.3. Electrochemical behavior of Iron(III)–DBC^{2-} adducts

The electrochemical features of the iron(III)–DBC^{2-} adducts **1**–**4** were investigated in methanol solution by employing cyclic (CV) and differential pulse voltammetry (DPV) on a stationary Pt electrode. All the four [Fe(L)(DBC)(CH_3OH)] adducts exhibit three electrochemical responses (Figs. 3 and 4), which are assigned to iron(III)/iron(II), DBSQ/DBC^{2-} and DBQ/DBSQ redox couples. The redox potentials of Fe(III)/Fe(II) couple fall in the more negative region −0.532 to −0.605 V (Table 2) due to strong coordination of the phenolate ligands and DBC^{2-} dianion and follow the trend **3** > **2** > **1** > **4**, reflecting an increase in interaction between catecholate anion and the iron(III) center along this series. Thus, upon incorporating the electron-releasing *tert*-butyl groups on the phenolate ring in **1** to obtain **3**, the Fe(III)/Fe(II) redox potential becomes more positive illustrating the weaker interaction of catecholate anion with iron(III) center. On the other hand, the incorporation of the electron-withdrawing –NO_2 group in **1** to obtain **4**, the Fe(III)/Fe(II) redox potential

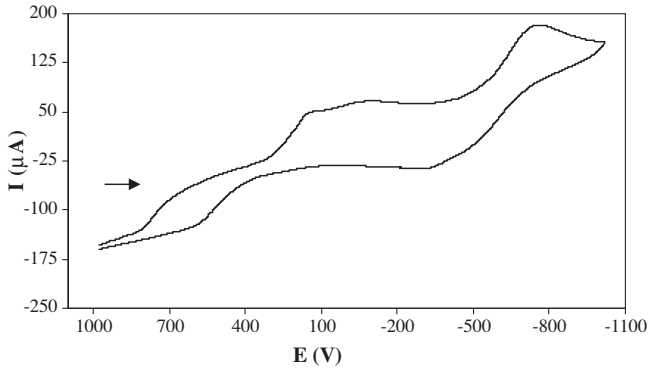

Fig. 3. Cyclic voltammogram of **2** in methanol solution at 25 °C. Supporting electrolyte: 0.1 M TBAP. Scan rate: 50 mV s^{-1}.

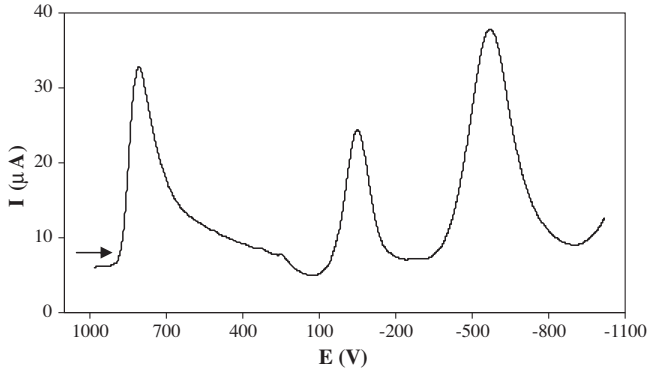

Fig. 4. Differential pulse voltammogram of **2** in methanol solution at 25 °C. Supporting electrolyte: 0.1 M TBAP. Scan rate: 5 mV s^{-1}.

Table 2
Electrochemical data[a] for [Fe(L)(DBC)(CH_3OH)] in methanol at 25 ± 0.2 °C using a scan rate of 50 mV/s (CV) and in 5 mV/s (DPV).

Complex	$E_{1/2}$ (V)		Process
	CV	DPV	
[Fe(L1)(DBC)(CH_3OH)]	–	0.916	DBQ → DBSQ
	−0.023	−0.027	DBSQ → DBC
	–	−0.587	Fe^{III} → Fe^{II}
[Fe(L2)(DBC)(CH_3OH)]	–	0.826	DBQ → DBSQ
	−0.038	−0.034	DBSQ → DBC
	–	−0.552	Fe^{III} → Fe^{II}
[Fe(L3)(DBC)(CH_3OH)]	–	0.815	DBQ → DBSQ
	−0.040	−0.044	DBSQ → DBC
	–	−0.532	Fe^{III} → Fe^{II}
[Fe(L4)(DBC)(CH_3OH)]	–	0.924	DBQ → DBSQ
	0.043	0.040	DBSQ → DBC
	–	−0.605	Fe^{III} → Fe^{II}

[a] Potential measured vs. Ag(s)/$AgNO_3$ (0.01 M, 0.10 M TBAP); add 0.544 V to convert to NHE.

becomes more negative illustrating the stronger interaction of DBC^{2-} with iron(III) center. This means that the electron-transfer [57] from catecholate adducts to dioxygen is thermodynamically more unfavorable in **4** than in **1**–**3**, due to the higher covalency of iron(III)–DBC^{2-} bonds. The redox potentials of the DBSQ/DBC^{2-} couple (−0.040 to +0.043 V) for the [Fe(L)(DBC)(CH_3OH)] is higher than that for the free DBSQ/DBC^{2-} couple (E_{pc}, −1.274 V) [30], revealing the significant stabilization of coordinated DBC^{2-} anion toward oxidation. They follow the trend **3** < **2** < **1** < **4**, revealing that the stabilization of coordinated DBC^{2-} toward oxidation increases along the series. On incorporating *tert*-butyl groups on the phenolate

ring in **1** to obtain **3**, the electron density on iron(III) increases leading to a weaker iron (III)–DBC^{2-} interaction and so the DBSQ/DBC^{2-} redox couple is located in the more negative region. Similarly, on incorporating two methyl groups on the phenolate ring to obtain **2**, the DBSQ/DBC^{2-} redox couple is slightly shifted to the negative region. The incorporation of electron-withdrawing $-NO_2$ group shifts the DBSQ/DBC^{2-} redox couple to a more positive value revealing that electron-transfer from catecholate adducts to dioxygen is made difficult and hence less reactive than that in **1**. The trend in the redox potentials of DBQ/DBSQ couple (0.815-0.924 V) is the same as that observed for DBSQ/DBC^{2-} couple. It may be noted that all the observed trends in $E_{1/2}$ values of DBSQ/DBC^{2-} couple are consistent with the above spectral results.

3.4. Dioxygenase activity of Iron(III)–DBC^{2-} adducts

The iron(III)–catecholate adducts **1**–**4** were reacted with molecular oxygen in methanol solution. The disappearance of the low-energy catecholate-to-iron(III) LMCT band (Fig. 5) on oxygenation exhibits pseudo-first order kinetics as judged from the linearity of the [1 + log(absorbance)] versus time plot and the value of k_{obs} was calculated from the slope of the plot (Fig. 6). The second order rate constant was then derived (Table 3) by using the equation,

$$k_{O_2} = k_{obs}/[O_2]$$

The products of cleavage of H_2DBC in methanol solvent (Table 3) are identified (**5**–**8**, Scheme 3) by GC–MS and ^1H NMR techniques and quantified by GC analysis.

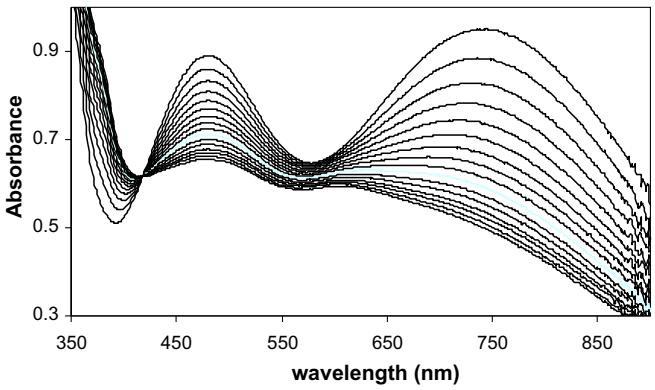

Fig. 5. Progress of the reaction of adduct [Fe(L2)(DBC)(CH_3OH)] with O_2 in methanol solution. The disappearance of the DBC^{2-}-to-iron(III) charge-transfer band is monitored.

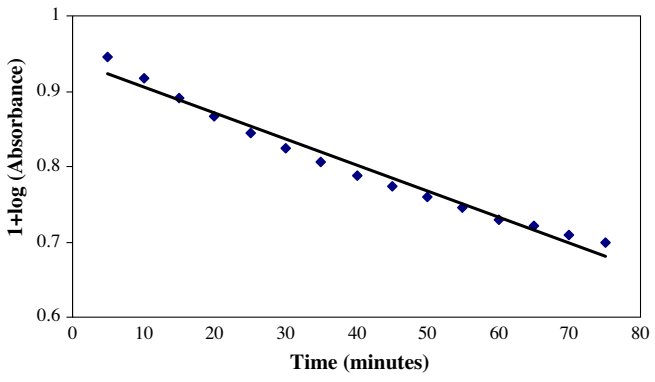

Fig. 6. Plot of [1 + log(absorbance)] versus time for the reaction of adduct [Fe(L2)(DBC)] with O_2 at 25 °C in methanol solution. The Concentration of adduct, 4×10^{-4} M.

Table 3
Kinetic data for oxidative cleavage of DBC^{2-} in iron(III)–DBC^{2-} adducts in methanol and the cleavage products.

Complex	k_{O_2} M^{-1} s^{-1} ($\times 10^{-2}$)	Cleavage products			
		Extradiol	Intradiol	Total	*E*/*I* ratio
[Fe(L1)(DBC)(CH_3OH)]	5.03	35.3 (**5**, **6**)	45.7 (**7**, **8**)	81.0	0.8
[Fe(L2)(DBC)(CH_3OH)]	6.26	28.6 (**5**, **6**)	62.6 (**7**, **8**)	91.2	0.5
[Fe(L3)(DBC)(CH_3OH)]	7.18	20.3 (**5**, **6**)	70.1 (**7**, **8**)	90.4	0.3
[Fe(L4)(DBC)(CH_3OH)]	5.50	55.9 (**5**, **6**)	28.3 (**7**, **8**)	84.2	1.9

The catecholate adducts **1**–**4** were reacted with dioxygen over 48 h ($t_{1/2}$, 1.3–1.8 h) to afford 80–90% of cleavage products and the remaining 10–20% is detected as H_2DBC. The formation of both intradiol (I, 38–70%) and extradiol (E, 20–46%) cleavage products (Scheme 3, Table 3) is observed with the product selectivity (E/I) falling in the range 0.3–1.2. This is interesting because only intradiol cleavage products (97%) have been observed previously for [Fe(L1)(DBC)(DMF)] in DMF solvent [29]. Also, the yield of extradiol cleavage products follow the trend **3** (20.3) < **2** (28.6) < **1** (35.3) < **4** (55.9%) whereas that of intradiol cleavage products follow the reverse trend **3** (70.1) > **2** (62.6) > **1** (45.7) > **4** (38.3%). All these observations can be illustrated by invoking both substrate [19,20,58,59] and oxygen activation [60,61] mechanisms proposed for the enzymes. It is well-known that substrate activation pathway, which involves the attack of dioxygen on the activated substrate, that is, the semiquinonate radical of iron(II)–DBSQ species, leads to the formation of intradiol cleavage products. On the other hand, dioxygen activation mechanism, which involves the attack of dioxygen on the vacant or solvent coordinated site on iron(II) bound to catecholate, leads to the formation extradiol cleavage products. Also, in both the cases the same alkylperoxoiron(III) intermediate (Scheme 4) in which the iron(III) center is bridged with the semiquinonate carbon through a peroxy group. An acyl migration in this alkylperoxoiron(III) intermediate gives intradiol cleavage products while alkenyl migration yields extradiol cleavage products. Very recently, the key peroxide intermediate and the O_2 adduct precursor and the product complex successor to the substrate-alkylperoxo-Fe^{2+} intermediate are found [57] to be simultaneously present in the X-ray crystal structures of different subunits of the homoprotocatechuate 2,3-dioxygenase enzyme reacted with 4-nitrocatechol as the substrate. Upon incorporating the electron-releasing *tert*-butyl group on the phenolate ring in **1** to obtain **3**, the electron density on iron(III) center increases illustrating that O_2 attack on the activated substrate rather than on the iron center is facilitated leading to the formation of intradiol cleavage products more for **3** (70.1%) than for **1** (45.7%). Similarly, on incorporating the electron-releasing methyl group in **1** to obtain **2**, only a lower increase in intradiol cleavage (62.6%) products is observed, as expected. On the other hand, on incorporating the electron-withdrawing $-NO_2$ group on the phenolate ring in **1** to obtain **4**, the electron density on iron(III) center decreases leading to facilitate O_2 attack on the iron center and hence the yield of extradiol cleavage product is higher for **4** (55.9%) than for **1**–**3**. Thus, for the present catecholate adducts, the Lewis basicity of the primary ligand, as modified by the substituents on the phenolate ring, dictates the choice of substrate or oxygen activation mechanism, and hence the regioselectivity of catechol cleavage.

It may be noted that the redox potential of DBC^{2-}/DBSQ couple is more positive for **4** than for others illustrating that the removal of electron from or the oxidation of the bound catecholate is difficult; in other words, substrate activation pathway is not facilitated

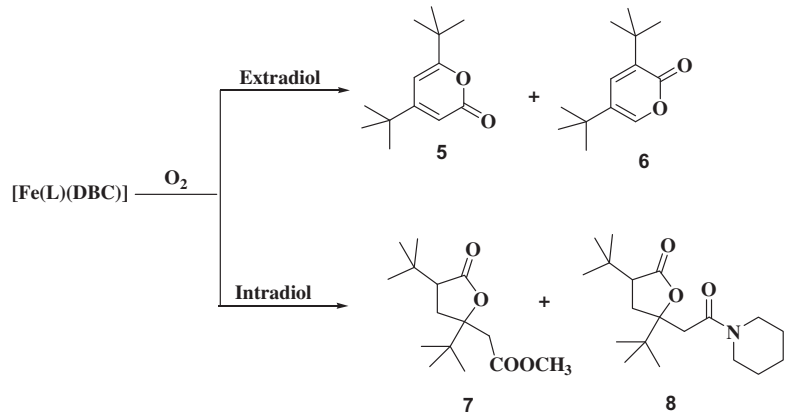

Scheme 3. Products of catechol cleavage of H_2DBC of [Fe(L)(DBC)] adducts using molecular oxygen: 4,6-di-*tert*-butyl-2*H*-pyran-2-one (**5**), 3,5-di-*tert*-butyl-2*H*-pyran-2-one (**6**), methyl-2-(2,4-di-*tert*-butyl-5-oxo-tetrahydrofuran-2-yl)acetate (**7**), 3,5-di-*tert*-butyl-5-(2-oxo-2-(piperidin-1-yl)ethyl)-dihydrofuran-2(3*H*)-one (**8**).

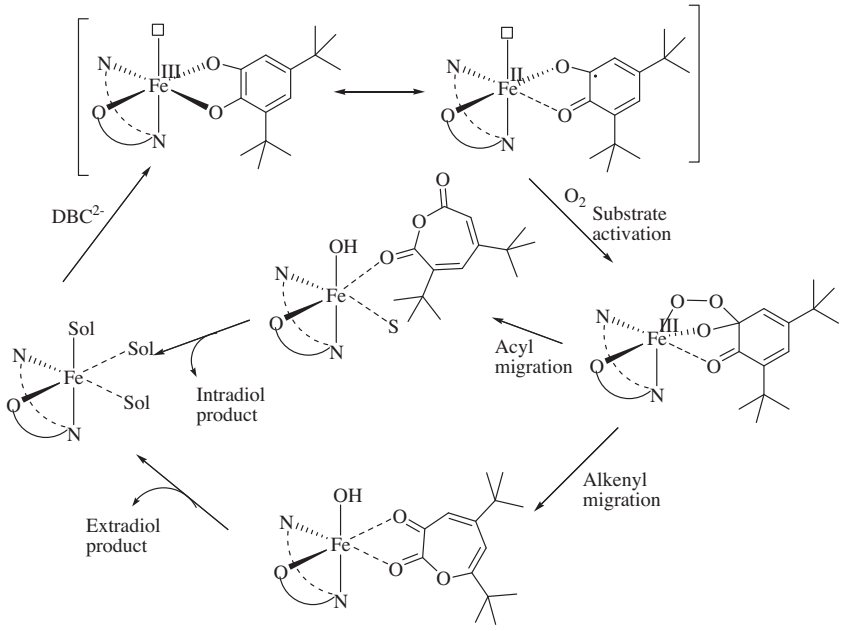

Scheme 4. Proposed mechanisms for both extra- and intradiol cleavage products.

and oxygen activation is encouraged leading to extradiol cleavage pathway. Also, the higher negative redox potential of DBC^{2-}/DBSQ couple for **4** encourages oxygen attack on the substrate leading to facilitate intradiol rather than extradiol cleavage product. Also, it is to be noted that the adduct [Fe(L1)(DBC)(DMF)] [29] and the adducts of the type [Fe(L)(DBC)Cl], where L is a tridentate 3N ligand, afford only intradiol cleavage products in DMF solvent [27,42,43]. This type of selective formation of intradiol cleavage products is because the substitution of strongly coordinated DMF solvent by molecular oxygen is made difficult and hence the substrate activation mechanism is preferred in DMF solvent.

The second order rate constants observed for the [Fe(L)(DBC)(CH_3OH)] adducts **1**–**4** fall in the range $5.0–7.2 \times 10^{-2}\ M^{-1}\ s^{-1}$ (Table 3), which corresponds to the involvement of both intradiol and extradiol cleavage mechanisms to different extents. The reaction rate constants follow the trend **3** > **2** > **1** < **4**. Upon incorporating the electron-releasing *tert*-butyl groups on the phenolate ring in **1** to obtain **3**, the electron density on iron(III) center increases and hence the rate of dioxygenation to give extradiol product would be expected to decrease, but, in contrast, an increase in reaction rate is observed, which is mainly because the intradiol cleavage pathway is facilitated more. Similarly, on incorporating the electron-releasing methyl groups in **1** to obtain **2**, only a slight increase in reaction rate is observed. On the other hand, on incorporating the electron-withdrawing group $–NO_2$ in **1** to obtain **4**, though most of the adduct species follow the extradiol cleavage (dioxygen activation) path way, the rate of the reaction is increased mainly due to the higher Lewis acidity of iron(III) center conferred upon by nitro group and hence the enhanced O_2 attack [20,23,45,62]. Thus the nature of substituents on the phenolate ring of the ligands controls the reaction rate as well as product selectivity.

4. Conclusions

A few catecholate adducts of iron(III) complexes of facially coordinating tridentate phenolate ligands with different ring substituents have been isolated and studied as models for enzyme-substrate adducts of catechol dioxygenase enzymes. The adducts show two $DBC^{2-} \rightarrow$ iron(III) LMCT bands in the visible region, which are similar to those observed for the enzyme–substrate

adducts under steady state conditions. Interestingly, the incorporation of an electron-releasing substituent on the phenolate ring shifts the energy of the low-energy LMCT band to higher energy and facilitates regioselective intradiol cleavage of catechol. On the other hand, the incorporation of an electron-withdrawing substituent shifts the LMCT band to lower energy and facilitates the regioselective extradiol cleavage of catechol.

Acknowledgements

We sincerely thank the Council of Scientific and Industrial Research, New Delhi for Senior Research Fellowship to K.V. This work is supported also by the Indo-French Centre (IFCPAR) (Scheme No. IFC/A/4109-1/2009/993). Professor M. Palaniandavar is a recipient of DST Ramanna Fellowship (Scheme No. SR/S1/RFIC-01/2007 and SR/S1/RFIC-01/2010). We thank Prof. Krishna P. Kaliappan, Indian Institute of Technology Bombay, Mumbai, for ESI-MS analysis.

References

[1] P.S. Phale, A. Basu, P.D. Majhi, J. Deveryshetty, C. Vamsee-Krishna, R. Shrivastava, J. Integ. Biol. 11 (2007) 252.
[2] O. Hayaishi, M. Katagiri, S. Rothberg, J. Am. Chem. Soc. 77 (1955) 5450.
[3] Y. Kojima, N. Itada, O. Hayaishi, J. Biol. Chem. 236 (1961) 2223.
[4] O. Hayaishi, Bacteriol. Rev. 30 (1966) 720.
[5] D.H. Ohlendorf, J.D. Lipscomb, P.C. Weber, Nature 336 (1988) 403.
[6] D.H. Ohlendorf, A.M. Orville, J.D. Lipscomb, J. Mol. Biol. 244 (1994) 586.
[7] M.W. Vetting, D.H. Ohlendorf, Structure 8 (2000) 429.
[8] A.M. Orville, J.D. Lipscomb, D.H. Ohlendorf, Biochemistry 36 (1997) 10052.
[9] M.W. Vetting, C.A. Earhart, D.H. Ohlendorf, J. Mol. Biol. 236 (1994) 372.
[10] T.E. Elgren, A.M. Orville, K.A. Kelly, J.D. Lipscomb, D.H. Ohlendorf, L. Que Jr., Biochemistry 36 (1997) 11504.
[11] S. Han, L.D. Eltis, K.N. Timmis, S.W. Muchmore, J.T. Bolin, Science 270 (1995) 976.
[12] K. Sugimoto, T. Senda, H. Aoshima, E. Masai, M. Fukuda, Y. Mitsui, Structure 7 (1999) 953.
[13] A. Kita, S.I. Kita, I. Fujisawa, K. Inaka, T. Ishida, K. Horiike, M. Nozaki, K. Miki, Structure 7 (1998) 25.
[14] F.H. Vaillancourt, C.J. Barbosa, T.G. Spiro, J.T. Bolin, M.W. Blades, R.F.B. Turner, L.D. Eltis, J. Am. Chem. Soc. 124 (2002) 2485.
[15] Y. Uragami, T. Senda, K. Sugimoto, N. Sato, V. Nagarajan, E. Masai, M. Fukuda, Y. Mitsui, J. Inorg. Biochem. 83 (2001) 269.
[16] N. Sato, Y. Uragami, T. Nishizaki, Y. Takahashi, G. Sazaki, K. Sugimoto, T. Nonaka, E. Masai, M. Fukuda, T. Senda, J. Mol. Biol. 321 (2002) 621.
[17] T.D.H. Bugg, G. Lin, Chem. Commun. 11 (2001) 941.
[18] M. Costas, M.P. Mehn, M.P. Jensen, L. Que Jr., Chem. Rev. 104 (2004) 939.
[19] D.D. Cox, L. Que Jr., J. Am. Chem. Soc. 110 (1988) 8085.
[20] H.G. Jang, D.D. Cox, L. Que Jr., J. Am. Chem. Soc. 113 (1991) 9200.
[21] R. Viswanathan, M. Palaniandavar, T. Balasubramanian, P.T. Muthiah, J. Chem. Soc., Dalton Trans. (1996) 2519.
[22] W.O. Koch, V. Schünemann, M. Gerdan, A.X.H. Trautwein, J. Chem. Eur. J. 4 (1998) 1255.
[23] R. Viswanathan, M. Palaniandavar, T. Balasubramanian, P.T. Muthiah, Inorg. Chem. 37 (1998) 2943.
[24] N. Raffard, R. Carina, A.J. Simaan, J. Sainton, E. Riviere, L. Tchertanov, S. Bourcier, G. Bouchoux, M. Delroisse, F. Banse, J.J. Girerd, Eur. J. Inorg. Chem. (2001) 2249.
[25] M. Velusamy, M. Palaniandavar, R. Srinivasagopalan, G.U. Kulkarni, Inorg. Chem. 42 (2003) 8283.
[26] M. Velusamy, R. Mayilmurugan, M. Palaniandavar, Inorg. Chem. 43 (2004) 6284.
[27] M. Velusamy, R. Mayilmurugan, M. Palaniandavar, J. Inorg. Biochem. 99 (2005) 1032.
[28] M. Pascaly, M. Duda, F. Schweppe, K. Zurlinden, F.K. Muller, B. Krebs, J. Chem. Soc., Dalton Trans. (2001) 828.
[29] S. Ogo, R. Yamahara, T. Funabiki, H. Masuda, Y. Watanabe, Chem. Lett. (2001) 1062.
[30] R. Mayilmurugan, H. Stoeckli-Evans, M. Palaniandavar, Inorg. Chem. 47 (2008) 6645.
[31] T. Funabiki, A. Mizoguchi, T. Sugimoto, S. Tada, M. Tsugi, H. Sakamoto, S. Yoshida, J. Am. Chem. Soc. 108 (1986) 2921.
[32] A. Dei, D. Gatteschi, L. Pardi, Inorg. Chem. 32 (1993) 1389.
[33] G. Lin, G. Reid, T.D.H. Bugg, J. Am. Chem. Soc. 123 (2001) 5030.
[34] M. Ito, L. Que Jr., Angew. Chem., Int. Ed. Engl. 36 (1997) 1342.
[35] D.-H. Jo, L. Que Jr., Angew. Chem., Int. Ed. 39 (2000) 4284.
[36] J.H. Lim, T.H. Park, H.-J. Lee, K.-B. Lee, H.G. Jang, Bull. Korean Chem. Soc. 20 (1999) 1428.
[37] Y.-M. Chiou, L. Que Jr., Inorg. Chem. 34 (1995) 3577.
[38] R. Mayilmurugan, E. Suresh, M. Palaniandavar, Inorg. Chem. 46 (2007) 6038.
[39] T. Dhanalakshmi, M. Bhuvaneshwari, M. Palaniandavar, J. Inorg. Biochem. 100 (2006) 1527.
[40] P.C.A. Bruijnincx, M. Lutz, A.L. Spek, W.R. Hagen, B.M. Weckhuysen, G. Koten, R.J.M. Klein Gebbink, J. Am. Chem. Soc. 129 (2007) 2275.
[41] M. Wagner, C. Limberg, T. Tietz, Chem. Eur. J. 15 (2009) 5567.
[42] K. Visvaganesan, R. Mayilmurugan, E. Suresh, M. Palaniandavar, Inorg. Chem. 46 (2007) 10294.
[43] K. Sundaravel, T. Dhanalakshmi, E. Suresh, M. Palaniandavar, Dalton Trans. (2008) 7012.
[44] T. Dhanalkshmi, E. Suresh, M. Palaniandavar, Dalton Trans. (2009) 8317.
[45] T. Ogihara, S. Hikichi, M. Akita, Y. Moro-oka, Inorg. Chem. 37 (1998) 2614.
[46] R. Viswanathan, M. Palaniandavar, J. Chem. Soc., Dalton Trans. (1995) 1259.
[47] N. Anitha, M. Palaniandavar, Dalton Trans. 39 (2010) 1195.
[48] P. Barbaro, C. Bianchini, C. Mealli, A. Meli, J. Am. Chem. Soc. 113 (1991) 3181.
[49] T. Yajima, Y. Shimazaki, N. Ishigami, A. Odani, O. Yamauchi, Inorg. Chim. Acta 337 (2002) 193.
[50] E.Y. Tshuva, I. Goldberg, M. Kol, Z. Goldschmidt, Inorg. Chem. 40 (2001) 4263.
[51] A. Harold, F.L. Goodwin, J. Am. Chem. Soc. 82 (1960) 5013.
[52] F. Thomas, O. Jarjayes, H. Jamet, S. Hamman, E. Saint-Aman, C. Duboc, J. Pierre, Angew. Chem., Int. Ed. 43 (2004) 594.
[53] H. Mishra, R. Mukherjee, J. Organomet. Chem. 692 (2007) 3248.
[54] Z. Zheng, G. Zhao, R. Fablet, M. Bouyahyi, C.M. Thomas, T. Roisnel, O. Casagrande Jr., J. Carpentier, New J. Chem. 32 (2008) 2279.
[55] M. Kiran Kumar, S. Prabhakar, M. Ravi Kumar, T. Jehadeshwar Reddy, S. Premsingh, S. Rajagopal, M. Vairamani, Rapid. Commun. Mass Sp. 18 (2004) 1103.
[56] R. Mayilmurugan, K. Visvaganesan, E. Suresh, M. Palaniandavar, Inorg. Chem. 48 (2009) 8771.
[57] E.G. Kovaleva, J.D. Lipscomb, Science 316 (2007) 453.
[58] M.Y.M. Pau, J.D. Lipscomb, E.I. Solomon, Proc. Natl. Acad. Sci. USA 104 (2007) 18355.
[59] Jr.L. Que, J.D. Lipscomb, E. Munck, J.M. Wood, Biochim. Biophys. Acta 485 (1977) 60.
[60] E.I. Solomon, T.C. Brunold, M.I. Davis, J.N. Kemsley, S.-K. Lee, N. Lehnert, F. Neese, A.J. Skulan, Y.-S. Yang, J. Zhou, Chem. Rev. 100 (2000) 235.
[61] E.I. Solomon, A. Decker, N. Lehnert, Proc. Natl. Acad. Sci. USA 100 (2003) 3589.
[62] M. Palaniandavar, R. Viswanathan, Proc. Indian Acad. Sci., Chem. Sci. 108 (1996) 235.